

Asymmetric electromagnetic wave transmission of linear polarization via polarization conversion through chiral metamaterial structures

Ci Huang, Yijun Feng,* Junming Zhao, Zhengbin Wang, and Tian Jiang

Department of Electronic Engineering, School of Electronic Science and Engineering, Nanjing University, Nanjing 210093, China

(Received 1 March 2012; published 16 May 2012)

In this paper a kind of chiral metamaterial structure is proposed that can achieve asymmetric transmission for forward and backward propagations of linearly polarized electromagnetic (EM) waves. We first give a theoretical analysis on a kind of bilayered metamaterial structure with specific structure asymmetry that enables the asymmetric EM wave transmission *only* for linear polarization. Then by constructing a proof-of-concept metamaterial sample with twisted split ring resonator patterns on both sides of a dielectric slab, we demonstrate substantial asymmetric transmission for linear polarizations, but none for circular polarizations through full-wave simulation and measurement at microwave frequency. Strong optical activity is found in the chiral metamaterial indicating that the intriguing asymmetric transmission is caused by the directional difference in cross polarization conversion. By scaling down the structure, the proposed concept could be utilized in other frequency bands, such as terahertz and optical range.

DOI: [10.1103/PhysRevB.85.195131](https://doi.org/10.1103/PhysRevB.85.195131)

PACS number(s): 41.20.Jb, 42.25.Ja, 78.20.Ci, 78.67.Pt

I. INTRODUCTION

Asymmetric transmission of electromagnetic (EM) waves is normally associated with the presence of a static magnetization of the medium which breaks the reciprocity of the EM wave-matter interaction. This phenomenon is quite useful in realizing nonreciprocal EM devices such as isolators and circulators, especially in the microwave range.¹ However, these devices are usually heavy and involve magnetic bulk materials, not suitable for microwave circuit miniaturization.

During the past several years, metamaterial as a kind of artificial material has attracted an enormous amount of interest due to its intriguing EM responses that cannot be obtained with existing natural materials. Initial studies on metamaterials were limited to rather simple unit-cell structures with high symmetry.^{2,3} Recently, more sophisticated metamaterials with inclusions of symmetry-broken chiral structures have been proposed that could be used to achieve many customized functionalities, such as the negative refraction.⁴⁻⁶ Since the mirror symmetry of the unit-cell structures is broken either in the propagation direction or in the perpendicular plane, these chiral metamaterials could be utilized to manipulate the polarization states of EM waves and have shown novel features, such as giant optical activity,⁷⁻⁹ polarization transformation,¹⁰⁻¹² and circular or elliptical dichroism.^{13,14} Moreover, asymmetric EM wave transmission of circular polarizations has been reported in planar chiral metamaterials, where the partial conversion of the incident EM wave into one of the opposite handedness is asymmetric for the opposite directions of propagation.¹⁴⁻¹⁷ This asymmetric transmission phenomenon is irrelevant to the nonreciprocity of the Faraday effect in magneto-optical media,¹⁸ but originates from the interaction of EM radiation with the structural two-dimensional (2D) chirality in the metamaterials. However, the asymmetric transmission is absent for linear polarization in these planar structures. By introducing symmetry broken along the propagation direction in the metamaterial structure, asymmetric transmission of linear polarization can be obtained and experimentally demonstrated in the optical regime.^{19,20}

In this paper, we report the demonstration of asymmetric transmission for *linearly* polarized EM waves *only*. Such phenomenon is more interesting in the application for designing microwave devices. We first present theoretical study on how to construct specific chiral metamaterial to achieve asymmetric transmission of linear polarizations. Then based on the design rule, we propose a chiral structure composed of 90° twisted split ring resonators (SRRs) on both sides of a dielectric slab which verifies the only asymmetric transmission of linear polarizations. We will present the design, simulation, and the measurement of the chiral metamaterial structure, which show asymmetric EM wave transmission of a certain linearly polarized EM wave in the microwave band.

II. THEORETICAL ANALYSIS

Let us first consider the theoretical analysis of the EM wave propagation through a certain slab of uniform chiral medium. Asymmetric transmission of EM waves in the chiral metamaterial is usually caused by the partial polarization conversion of the incident EM radiation into one of the opposite polarization, which is asymmetric for the opposite directions of propagation.¹⁵ We consider an incoming plane wave propagating along the positive z direction, with electric field as

$$\mathbf{E}^{in}(\mathbf{r}, t) = \begin{pmatrix} I_x \\ I_y \end{pmatrix} e^{i(kz - \omega t)}, \quad (1)$$

where ω , k , I_x , and I_y represent the frequency, wave vector, and complex amplitudes, respectively. The transmitted electric field through the slab can be then described as

$$\mathbf{E}^{tr}(\mathbf{r}, t) = \begin{pmatrix} T_x \\ T_y \end{pmatrix} e^{i(kz - \omega t)}. \quad (2)$$

To understand better the cross-polarization conversion based on the chirality of the metamaterial structure, we invoke the transmission matrix expression for the EM fields $\mathbf{E}_i^{tr} = t_{ij} \mathbf{E}_j^{in}$, which relates the incident and the transmitted

electric fields in terms of linearly polarized components. The subscripts i and j correspond to the polarization states of the transmitted and the incident waves, which could be either x or y linear polarization. The matrix, which is usually called the Jones matrix \mathbf{T} , is then described as

$$\begin{pmatrix} T_x \\ T_y \end{pmatrix} = \begin{pmatrix} t_{xx} & t_{xy} \\ t_{yx} & t_{yy} \end{pmatrix} \begin{pmatrix} I_x \\ I_y \end{pmatrix} = \mathbf{T}_{\text{lin}}^f \begin{pmatrix} I_x \\ I_y \end{pmatrix}. \quad (3)$$

The superscript f and subscript lin indicate the forward propagation (along $+z$ direction) and a special linear base, respectively. If the medium does not contain magneto-optical material, the reciprocity theorem can be applied and the transmission matrix \mathbf{T}^b for propagation in the backward direction ($-z$ direction) can be derived as¹⁹

$$\mathbf{T}_{\text{lin}}^b = \begin{pmatrix} t_{xx} & -t_{yx} \\ -t_{xy} & t_{yy} \end{pmatrix}. \quad (4)$$

When the propagation direction is reversed, the off-diagonal elements t_{xy} and t_{yx} not only interchange their values, but also get an additional 180° phase shift. For a circular polarization basis, the \mathbf{T} matrix that connecting the incident and the transmitted circularly polarized components can be described by changing the base vectors from linear to circular states, resulting in

$$\begin{aligned} \mathbf{T}_{\text{circ}}^f &= \begin{pmatrix} t_{++} & t_{+-} \\ t_{-+} & t_{--} \end{pmatrix} \\ &= \frac{1}{2} \begin{pmatrix} t_{xx} + t_{yy} + i(t_{xy} - t_{yx}) & t_{xx} - t_{yy} - i(t_{xy} + t_{yx}) \\ t_{xx} - t_{yy} + i(t_{xy} + t_{yx}) & t_{xx} + t_{yy} - i(t_{xy} - t_{yx}) \end{pmatrix}, \end{aligned} \quad (5)$$

where indices $+$ and $-$ denote the right and the left circular polarizations propagating along the $+z$ direction, respectively.

The asymmetric transmission of either the linearly or the circularly polarized waves is usually characterized by the Δ parameter, which is defined as the difference between the transmittances in the two opposite propagation directions ($+z$ and $-z$).¹⁹ The asymmetric transmission parameter Δ for the linear (indicated with subscript lin and superscript x or y) or the circular polarizations (indicated with subscript circ and superscript $+$ or $-$) is then defined as

$$\Delta_{\text{lin}}^{(x)} = |t_{yx}|^2 - |t_{xy}|^2 = -\Delta_{\text{lin}}^{(y)}, \quad (6)$$

or

$$\Delta_{\text{circ}}^{(+)} = |t_{-+}|^2 - |t_{+-}|^2 = -\Delta_{\text{circ}}^{(-)}, \quad (7)$$

respectively.

If we require the asymmetric transmission for linear polarization only, from Eqs. (5)–(7) the transmission matrix elements should satisfy the following condition:

$$|t_{xy}| \neq |t_{yx}|, \quad (8a)$$

$$t_{xx} = t_{yy}. \quad (8b)$$

It has been pointed out that for a planar anisotropic chiral metamaterial, the mirror image of the unit cell coincides with that seen from the back side, therefore $t_{xy} = t_{yx}$, which ensures no asymmetric transmission of linear polarizations.¹⁹ So, to

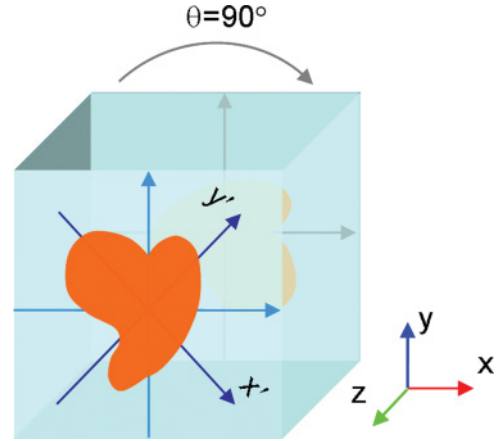


FIG. 1. (Color online) Schematics of the unit cell for the proposed chiral metamaterial.

obtain asymmetric transmission for linear polarization *only*, symmetry broken along the propagation direction is required, and specific structure asymmetry should be applied on the three dimensional (3D) unit cell to ensure the satisfactory solution of Eq. (8b).

Let us consider a specific kind of 3D chiral metamaterial structure with the unit cell schematically illustrated in Fig. 1. The meta-atom consists of two metallic layers parallel to the x - y plane sandwiching a dielectric layer. The metallic resonant structure in each layer has the same arbitrary pattern, however, the structure in the second layer has been rotated clockwise about the z axis with $\theta = 90^\circ$ and then flipped along the x axis regarding that in the first layer. Then we establish a new coordinate system (x', y', z') by rotating the (x, y, z) coordinate about the z axis with $\theta/2 = 45^\circ$. It is obvious that the resonant structures in the two layers are of 180° rotation symmetry with respect to the y' axis. Due to this specific symmetric arrangement of the meta-atom, the metamaterial looks exactly the same as a y' -polarized (or x' -polarized) wave propagating either forward (z direction) or backward ($-z$ direction) through the slab. Therefore, from Eqs. (3) and (4), we have

$$t_{x'y'} = -t_{y'x'}. \quad (9)$$

The transmission matrix in the (x', y', z') coordinate can be obtained through coordinate transformation from the \mathbf{T} matrix in the (x, y, z) coordinate, which can be expressed as

$$\begin{pmatrix} t_{x'x'} & t_{x'y'} \\ t_{y'x'} & t_{y'y'} \end{pmatrix} = \mathbf{C} \begin{pmatrix} t_{xx} & t_{xy} \\ t_{yx} & t_{yy} \end{pmatrix} \mathbf{C}^{-1}, \quad (10)$$

where \mathbf{C} is the Jacobi matrix for the coordinate rotation, and can be determined by

$$\mathbf{C} = \frac{\sqrt{2}}{2} \begin{pmatrix} 1 & -1 \\ 1 & 1 \end{pmatrix}. \quad (11)$$

Substituting Eqs. (9) and (11) into (10), we finally get $t_{xx} = t_{yy}$, which means that the condition for only asymmetric transmission of linear polarizations can be fulfilled by this specific kind of metamaterial structure.

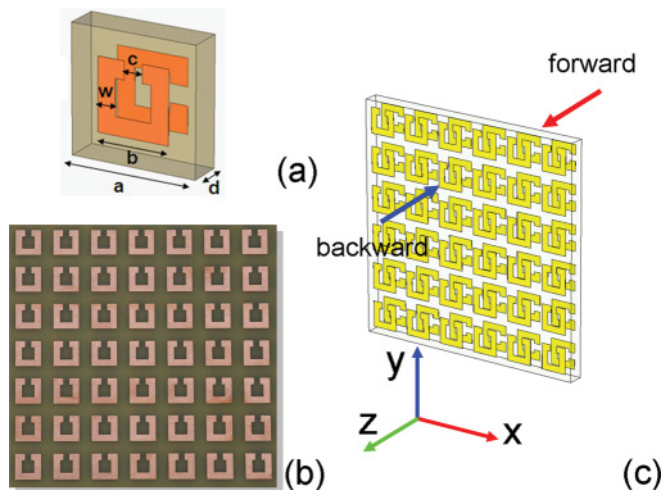


FIG. 2. (Color online) (a) Schematic of the chiral metamaterial unit cell. (b) Photograph of the fabricated sample slab, and (c) its orientation with the incident wave.

III. DESIGN AND CHARACTERISTICS

Based on the design rule described in the above section, we have constructed a proof-of-concept chiral metamaterial of double metallic layered structure. We employ simple square SRR as the resonant structure, which is often used in the chiral metamaterial design.^{7-9, 21-23} The unit cell consists of two metallic SRRs on both sides of a dielectric substrate twisted 90° to each other. Obviously, such structure accords with the design rule that allows it to achieve asymmetric transmission for linearly polarized EM waves only. In the design, the dielectric substrate is chosen as FR4 with a permittivity of 4.2, a loss tangent of 0.025, and a thickness of $d = 2.5$ mm, while the metallic layers on both sides are copper sheet with a thickness of $17 \mu\text{m}$. Figure 2(a) shows the schematic diagram of the metamaterial unit cell with a dimension of $12 \times 12 \text{ mm}^2$, while the whole slab sample is composed of 24×24 unit cells. The SRR patterns on both metallic layers are illustrated, which have an outer side length of $b = 8$ mm, a metallic wire width of $w = 2$ mm, and a gap of $c = 2$ mm. The twisted SRRs form a chiral structure and have strong strength to converse polarization of EM wave due to the electric and magnetic coupling between them. Figures 2(b) and 2(c) show the photograph of the fabricated sample and its orientation with the incident wave, respectively.

The proposed metamaterial slab has been first analyzed through full-wave EM simulations with a finite-difference time-domain (FDTD) based commercial tool. After the parameter optimization through the simulations, a sample slab (with outer dimension of $30 \times 30 \text{ cm}^2$) is then fabricated by printed circuit board technique and characterized through free space EM transmission measurement in a microwave anechoic chamber. Two linearly polarized horn antennas with Teflon lenses are used to feed and receive microwave signal at X band and a vector network analyzer (Agilent N5244A) is employed to measure the transmission coefficient. By changing the orientation of the two horn antennas, all four components of the EM wave transmission (the complex Jones matrix) for different polarizations have been measured.

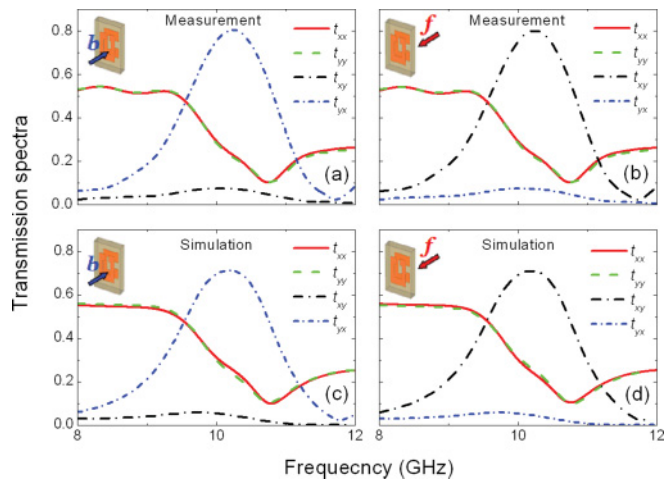


FIG. 3. (Color online) Measured (a), (b) and calculated (c), (d) transmission spectra of the four matrix components for backward (a), (c) and forward (b), (d) propagations.

Figure 3 shows the simulated and measured results of the four transmission matrix elements of the slab for propagation in forward ($+z$) and backward ($-z$) directions. The measurements and the simulations agree with each other well across the whole frequency range. As the frequency increases, the cross-polarization transmission t_{yx} experiences a resonant peak and reaches a maximum of around 0.8 at the frequency of 10.24 GHz, while the co-polarization transmission t_{xx} reduces to a minimum of about 0.1 at the frequency of 10.75 GHz, and t_{xy} is around a small value of 0.02 [Fig. 3(a)]. The remarkable difference between the two cross-polarization transmission components originates from the polarization conversion of the chiral structure. When the x -polarized (y -polarized) wave normally incidents into the structure along the $-z$ direction ($+z$ direction), the wave is well coupled to the structure through the gap in SRR and converted mostly to y polarization (x polarization) due to the cross coupling between two metallic layers when passing through the slab, while along the opposite direction, the x -polarized (y -polarized) wave can hardly be coupled to the structure, resulting in a weak transmission. According to Eq. (6), this leads to strong asymmetric transmission for linear polarization. In addition, Fig. 3 shows that when the propagation direction is reversed, the cross-polarization components t_{xy} and t_{yx} interchange with each other. As predicted in previous theoretical analysis, t_{xx} is exactly equal to t_{yy} , which could ensure zero asymmetric transmission of circular polarization waves for this particular chiral structure. The asymmetric transmission parameter Δ was calculated through Eqs. (6) and (7) for both linear polarizations and circular polarizations, and is illustrated in Fig. 4. When increasing the frequency, the value of parameter Δ for linear polarizations experiences a rapid increase and reaches the maximum of 0.64 at frequency of 10.24 GHz. However, due to the specific asymmetry in the structure, there is no asymmetric transmission for either the left (indicated by superscript “-”) or the right circular (indicated by superscript “+”) polarized waves as indicated in Fig. 4. This result provides a direct experimental conformation for the theoretic prediction in the previous section.

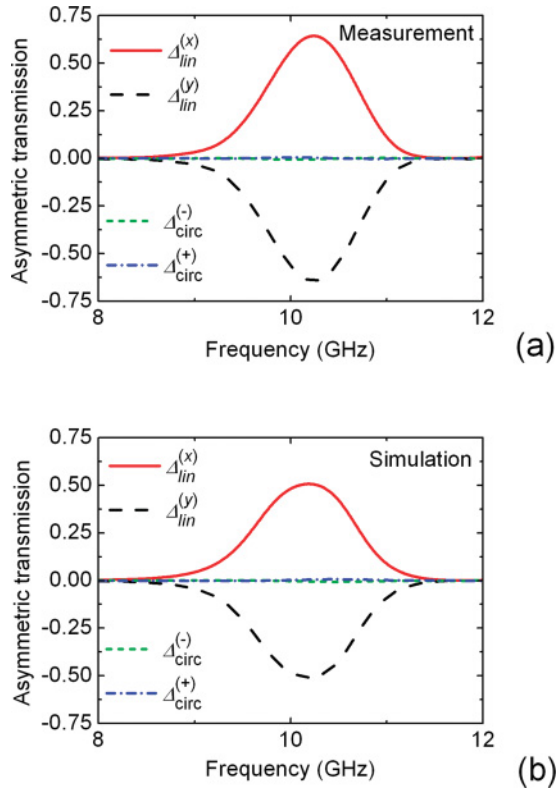


FIG. 4. (Color online) Asymmetric transmission parameter Δ for linear and circular polarization bases as determined by the measured (a) and calculated (b) data.

Due to the large asymmetric transmission parameter for the linear polarization in the proposed structure, the total transmission for a certain linearly polarized wave is quite different along opposite directions. We measured both the forward and backward *total* transmission (including both the co-polarization and cross-polarization) for an *x*-polarized wave and the result is shown in Fig. 5. The backward (along the $-z$ direction) transmission reaches to 70%, while the forward

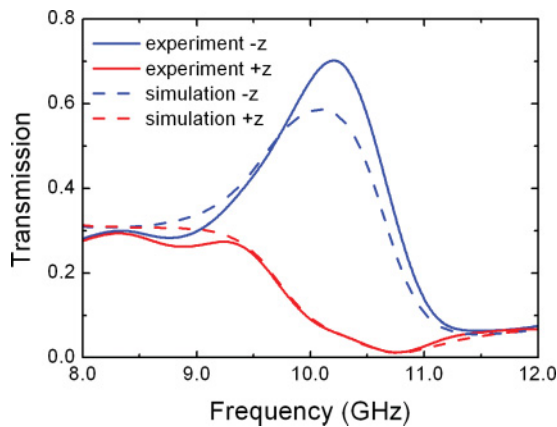


FIG. 5. (Color online) Measured (solid lines) and calculated (dashed lines) total transmission for an *x*-polarized incident wave along the forward ($+z$) and backward ($-z$) directions through the chiral metamaterial slab.

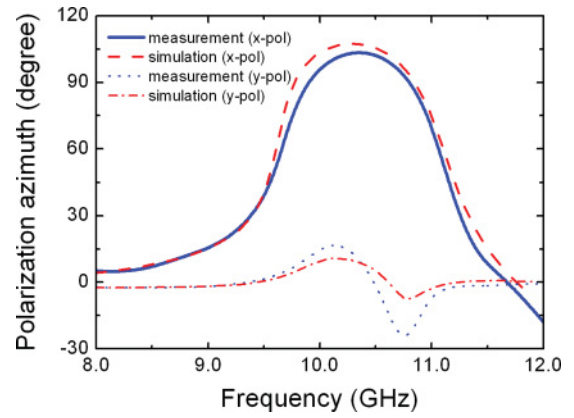


FIG. 6. (Color online) Polarization azimuth angle for an *x*-polarized or a *y*-polarized wave incident along the backward ($-z$) direction.

transmission is less than 10% around the resonant frequency (10.24 GHz).

The resonant coupling between the two SRRs also leads to strong optical activity accompanied with the asymmetric transmission in such chiral structure. Figure 6 shows the polarization azimuth of the transmitted wave for an *x*-polarized or a *y*-polarized incidence along the backward direction. Strong optical activity is found with large polarization azimuth for an *x*-polarized incidence, but much less value for a *y*-polarized incidence. As the frequency increases, the major polarization axis of the transmitted wave for an *x*-polarized incidence rotates counterclockwise rapidly toward the *y* axis. At around the frequency 9.78 GHz the polarization azimuth becomes 90° , and further reaches a maximum of 103° at 10.24 GHz. It indicated that the transmitted waves are mostly *y*-polarized within the frequency band ranging from 9.78 to 10.85 GHz.

To look into the mechanism of the asymmetric transmission that is associated with the chiral metamaterial, we have analyzed the EM wave evolution when propagating through the structure around the resonant frequency. Figure 7 illustrates three snapshots of electric-field distribution for an *x*-polarized wave passing through the slab backward or forward. These snapshots correspond to the electrical-field distributions for the wave in the incoming and outgoing regime, as well as inside the structure. As predicted in the theoretical study in Ref. 24, SRR structure exhibits interesting bi-anisotropic responses to EM waves. When the *x*-polarized wave incidents along the backward direction, the fundamental magnetic resonance mode of the first SRR can be excited efficiently at the resonant frequency with strong EM wave being coupled into the slab, and then the near-field coupling between the first and the second SRRs results in an obvious transmitted wave, but the polarization has been rotated by 90° [as indicated in Fig. 7(a)]. On the contrary, with an *x*-polarized wave incidence along the forward direction, it first hits the second SRR and its fundamental magnetic resonance cannot be well excited due to its orientation. Therefore the EM wave coupled into the slab is comparably weak, and results in a low level of transmission without polarization rotation [Fig. 7(b)]. This observation supports that the asymmetric transmission is

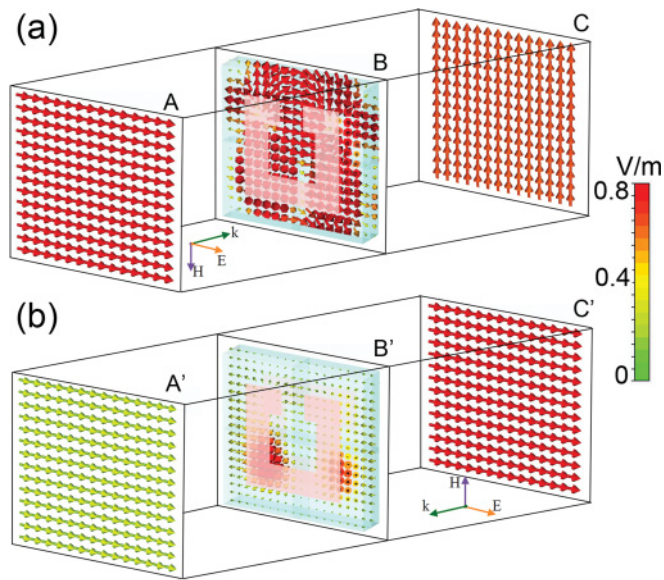


FIG. 7. (Color online) Calculated electric-field distributions at 9.78 GHz for an x -polarized wave incident along the backward (a) and forward (b) directions. Slices A, A' and C, C' are each 8 mm from the front and back sample surfaces, respectively, while slices B and B' are in the middle of the dielectric layer. The electric-field intensity, normalized to that of the incident wave, is illustrated by the color of the arrows.

caused by the resonant polarization convention together with the bi-anisotropic of SRRs with a difference in the coupling to orthogonal polarizations.

IV. CONCLUSIONS

In conclusion, we present a theoretical analysis of a kind of chiral metamaterial structure that could produce asymmetric EM transmission for linear polarization *only*. To verify the theoretical prediction, a proof-of-concept example of a chiral metamaterial slab has been composed with dielectric substrate sandwiched by two metallic layers with twisted SRR structures. By optimal design of the metamaterial structure through full-wave EM simulations, we fabricated and tested the structure at the microwave band. The experimental results have confirmed the strong asymmetric transmission of linear polarization along opposite propagation directions and demonstrated the optical activity associated with the chiral metamaterial. We believe that the proposed chiral metamaterial could find applications in designing compact and lightweight directional EM devices such as isolators and circulators. The strong optical activity in such structure could also be beneficial in designing microwave wave plate or other polarization control devices. By scaling down the proposed metamaterial structure, the concept could also be utilized to function at other frequency bands, such as millimeter wave, terahertz, or even optical range.

ACKNOWLEDGMENTS

The authors would like to thank the reviewer for stimulating suggestions. This work was supported by the National Nature Science Foundation (Grants No. 60990322, No. 60990320, No. 60801001, No. 61101011), and the Ph.D. Programs Foundation of Ministry of Education of China (Grant No. 20100091110036).

*yjfeng@nju.edu.cn

¹C. L. Hogan, *Rev. Mod. Phys.* **25**, 253 (1953).

²G. V. Eleftheriades and K. G. Balmain, *Negative-Refractive Metamaterials: Fundamental Principles and Applications* (Wiley-IEEE, New York, 2005).

³N. Engheta and R. W. Ziolkowski, *Metamaterials: Physics and Engineering Explorations* (Wiley-IEEE, New York, 2006).

⁴S. Zhang, Y. S. Park, J. Li, X. Lu, W. Zhang, and X. Zhang, *Phys. Rev. Lett.* **102**, 023901 (2009).

⁵B. Wang, J. Zhou, T. Koschny, and C. M. Soukoulis, *Appl. Phys. Lett.* **94**, 151112 (2009).

⁶E. Plum, J. Zhou, J. Dong, V. A. Fedotov, T. Koschny, C. M. Soukoulis, and N. I. Zheludev, *Phys. Rev. B* **79**, 035407 (2009).

⁷T. Q. Li, H. Liu, T. Li, S. M. Wang, F. M. Wang, R. X. Wu, P. Chen, S. N. Zhu, and X. Zhang, *Appl. Phys. Lett.* **92**, 131111 (2008).

⁸M. Decker, R. Zhao, C. M. Soukoulis, S. Linden, and M. Wegener, *Opt. Lett.* **35**, 1590 (2010).

⁹S. Engelbrecht, M. Wunderlich, A. M. Shuvaev, and A. Pimenov, *Appl. Phys. Lett.* **97**, 081116 (2010).

¹⁰J. Y. Chin, M. Lu, and T. J. Cui, *Appl. Phys. Lett.* **93**, 251903 (2008).

¹¹Y. Ye and S. He, *Appl. Phys. Lett.* **96**, 203501 (2010).

¹²J. Han, H. Q. Li, Y. C. Fan, Z. Y. Wei, C. Wu, Y. Cao, X. Yu, F. Li, and Z. S. Wang, *Appl. Phys. Lett.* **98**, 151908 (2011).

¹³M. Decker, M. W. Klein, M. Wegener, and S. Linden, *Opt. Lett.* **32**, 856 (2007).

¹⁴S. V. Zhukovsky, A. V. Novitsky, and V. M. Galynsky, *Opt. Lett.* **34**, 1988 (2009).

¹⁵V. A. Fedotov, P. L. Mladyonov, S. L. Prosvirnin, A. V. Rogacheva, Y. Chen, and N. I. Zheludev, *Phys. Rev. Lett.* **97**, 167401 (2006).

¹⁶V. A. Fedotov, A. S. Schwanecke, N. I. Zheludev, V. V. Khardikov, and S. L. Prosvirnin, *Nano Lett.* **7**, 1996 (2007).

¹⁷R. Singh, E. Plum, C. Menzel, C. Rockstuhl, A. K. Azad, R. A. Cheville, F. Lederer, W. Zhang, and N. I. Zheludev, *Phys. Rev. B* **80**, 153104 (2009).

¹⁸J. D. Jackson, *Classical Electrodynamics* (Wiley, New York, 1999).

¹⁹C. Menzel, C. Helgert, C. Rockstuhl, E. B. Kley, A. Tünnermann, T. Pertsch, and F. Lederer, *Phys. Rev. Lett.* **104**, 253902 (2010).

²⁰M. Kang, J. Chen, H. Cui, Y. Li, and H. Wang, *Opt. Express* **19**, 8347 (2011).

²¹N. Liu, H. Liu, S. Zhu, and H. Giessen, *Nat. Photon.* **3**, 157 (2009).

²²H. Liu, D. A. Genov, D. M. Wu, Y. M. Liu, Z. W. Liu, C. Sun, S. N. Zhu, and X. Zhang, *Phys. Rev. B* **76**, 073101 (2007).

²³X. Xiong, W. H. Sun, Y. J. Bao, M. Wang, R. W. Peng, C. Sun, X. Lu, J. Shao, Z. F. Li, and N. B. Ming, *Phys. Rev. B* **81**, 075119 (2010).

²⁴Lei Zhou and S. T. Chui, *Phys. Rev. B* **74**, 035419 (2006).